

Shape-controlled silver NPs for shape-dependent biological activities

Fatemeh Sadeghi¹, Abolfazl Yazdanpanah¹, Amirbabak Abrishamkar², Fatholah Moztafarzadeh¹, Arash Ramedani³, Sevda Pouraghaie¹, Haji Shirinzadeh⁴, Ali Samadikuchaksaraei^{5,6}, N.P.S. Chauhan⁷, L. Hopkinson⁸, Farshid Sefat⁸, Masoud Mozafari⁹ ✉

¹Biomaterials Group, Faculty of Biomedical Engineering (Centre of Excellence), Amirkabir University of Technology, P.O. Box 15875-4413 Tehran, Iran

²Mechanical Engineering Department, Coventry University, Coventry, UK

³Department of Nanoscience & Nanotechnology (INST), Sharif University of Technology, P.O. Box, 89694-14588 Tehran, Iran

⁴Semiconductor Department, Materials and Energy Research Center (MERC), P.O. Box 14155-4777 Tehran, Iran

⁵Cellular and Molecular Research Center, Iran University of Medical Sciences, Tehran, Iran

⁶Department of Tissue Engineering & Regenerative Medicine, Faculty of Advanced Technologies in Medicine, Iran University of Medical Sciences, Tehran, Iran

⁷Department of Chemistry, Faculty of Science, Co-Ed Wing, Bhupal Nobles University, Udaipur 313001, Rajasthan, India

⁸School of Engineering, Medical and Healthcare Technology Department, University of Bradford, Bradford BD7 1DP, UK

⁹Bioengineering Research Group, Nanotechnology and Advanced Materials Department, Materials and Energy Research Center (MERC), P.O. Box 14155-4777 Tehran, Iran

✉ E-mail: mozafari.masoud@gmail.com

Published in Micro & Nano Letters; Received on 15th December 2016; Revised on 3rd April 2017; Accepted on 4th April 2017

The most important issue during synthesis of nanoparticles (NPs) is to avoid particle agglomeration and adhesion. There have been several attempts to use special substances such as organic surfactants, polymers and stable ligands for this purpose. In this study, silver NPs were synthesised with and without gelatin macromolecules, as a green natural biopolymer, which resulted in NPs with varying shapes and sizes. The effect of morphological characteristics on the antibacterial and antifungal properties of the synthesised NPs were studied, by comparing Gram-negative (*Escherichia coli*) versus Gram-positive (*Staphylococcus aureus*) bacteria as well as fungi (*Candida albicans*) by calculation of minimal inhibition concentration value. The results corresponded well with the assumptions on the effects of shape and size on the antibacterial and antifungal properties of the studied NPs.

1. Introduction: Silver (Ag) has been proved to eliminate ~650 diseases caused by microorganisms. Although its mechanism is not completely understood, the disinfecting properties of Ag are greatly valued in medical and hygienic applications [1]. Nowadays, Ag is available in particles of <100 nanometres in diameter, referred to as Ag nanoparticles (Ag-NPs) or nanoAg, which demonstrate extraordinary physical, chemical and biological properties [2]. Ag-NPs bond with small hydrophobic glycoprotein groups on the surface of viruses inhibiting their binding with host cells. This substance has been proved to be effective for all DNA, RNA, coated and uncoated viruses tested. On studies with human immunodeficiency virus, it has been shown that 100% of this virus will be eliminated at 37°C in 3 h in the presence of Ag-NPs [3, 4]. Results from different journals indicate effects of different parameters such as shape, dimensions and solution stability on the antibacterial properties of this substance. For instance, when the size of NPs is ~10 nm, antibacterial properties are greatly enhanced [5]. In addition to antibacterial properties, Ag-NPs also have antifungal properties. They kill fungi by destroying their cell wall or puncturing their membrane and sometimes destroying parts of the membrane completely [6].

Currently, there are a number of methods for synthesising Ag-NPs which are all based on reduction of Ag ions in the presence of stabilising or coating agents, usually macromolecules [7, 8]. In a simple synthesising process of these particles, no specific energy source, for example, ultraviolet (UV) light, high-energy beams, ultrasonic waves is used. Most studies in this regard are focused on reduction of Ag ions with citrate ions as stabilisers and reducers [9]. Synthesis of Ag-NPs using polysaccharides and their derivatives as coating elements occurs in an aquatic environment. Sometimes, polysaccharides and their derivatives

act as both coating elements and reducers [10]. The most common members of polysaccharides family used for this purpose include chitosan, dextran, sodium alginate, gum arabic, gum acacia, chitosan lactate, carboxymethyl cellulose and carboxymethyl methyl [11]. The most important issue during synthesising NPs is to avoid particle agglomeration and adhesion [12]. As the growth of Ag-NPs can be controlled by stabilisers, by using different stabilisers, the shape and size of NPs could be modified. It is interesting that to date there has been no reports on synthesis of Ag-NPs using specific shapes of biopolymers.

In this Letter, Ag-NPs were synthesised by chemical and green synthesis methods. The effects of synthesis method and resultant shape of these NPs were assessed for their antibacterial and antifungal properties.

2. Materials and methods

2.1. Chemical synthesis of Ag-NPs: In this method, 2.0 g of polyvinyl stabiliser in 200 ml of water was stirred in a beaker on medium heat 40°C to solve completely. Then, Ag nitrate (AgNO₃) (10 ml, 1 M) was added to the solution reacting with the oxygen in water, resulting in dark Ag oxide which changes the colour of solution inducing errors in use of colour evaluation for estimation reaction end point. After a few minutes, to obtain spherical NPs, primary borohydride reviver was added causing sudden reduction and colour change to yellow followed by brown. This process was followed by addition of secondary reviver, oxygenated water 70%, which causes changes in shapes of NPs as well as colour spectrum from brown to red, pink, purple and finally blue which indicates the creation of triangular NPs with (111) planes and high effectiveness. To create repulsion between particles and obtain a stable colloid; therefore, trisodium

citrate was used. This process has to be carefully carried out, so as to obtain a stable and sustainable/renewable colloid. Factors such as water purity, thorough cleaning of beakers with distilled water, temperature, concentration metallic salts and reducing agents, and duration of reaction all affect the shape of NPs making shape and size control of particles a challenge.

2.2. Green synthesis of Ag-NPs using gelatin: In this method, biopolymers (including proteins and polysaccharides) are used as NPs stabilisers. Four different shapes (spherical, cubic, central structures: spherical, cubic and vice versa) of Ag-NPs were synthesised using this method without any reacting chemicals, where gelatin was used as a coating, forming and stabilising agent. In fact, UV from sunlight acts as a reducing agent of Ag ions at the presence of a stabilising agent, gelatin. The samples were prepared by dissolving 100 mg gelatin in 10 mg distilled water at 60°C, stirred in a beaker for 20 min and then AgNO₃ with different concentrations of 5, 10, 20 and 40 mg was added to the solutions, placed under sunlight (UV). The solution was placed on the stirrer for 2 h to obtain orange-brown solution of NPs. Gelatin (gel permeation chromatography data: Mw = 115,000 g/mol, Mn = 2800 g/mol, wide distribution) and AgNO₃ were purchased from Merck (Germany) and all the solutions were prepared using double distilled-deionised water.

2.3. Viable colony count (antifungal and antibacterial): The antifungal and antibacterial effects of NP ion release on bacterium and fungus were evaluated by determining the viable colony count after exposure of bacterial colonies (*Staphylococcus aureus* ATCC25923) and fungal cells (*Candida albicans* ATCC 90028) to powdered Ag-NP (as the coating) for a fixed period of time 24 h. For each test, a single bacterial or fungal colony was inoculated into a 120 ml starter Luria-Bertani culture medium (LB broth) separately and mixed for 1 min. Initial concentration for each was 5×10^5 colony forming units per millilitre for the strain. Afterwards, inoculated medium was divided into 39 \times 3 ml tubes. Viable colony count of powdered Ag-NP was performed for different masses of Ag-NP containing 0.2, 0.5, 1, 2, 3, 4, 5, 6, 7, 10 and 20 mg in tubes number 1–11, respectively. Organisms were incubated aerobically in an orbital shaker (200 rpm) at 37°C. The mixtures containing only the cell inoculum in LB were considered as negative controls. Number of colonies in each sample was counted after overnight incubation.

As for antifungal test, the minimal inhibition concentration (MIC) was estimated from the concentration of Ag-NP at which Ag inhibits the growth of fungal cells and the total viable cell numbers after 24 h of incubation remain at, or closely below, the initial inoculation value [13–15]. Whereas for antibacterial tests, suspension of bacteria in LB transferred into blood agar by a standard bacterial count calibrated loop. After 24 h incubation at 37°C on blood agar, the number of colonies was counted. The MIC was estimated from the concentration of Ag-NP at which Ag inhibits growth of the bacteria and the total viable cell numbers after 24 h of incubation remain at, or closely below, the initial inoculation value [16–18].

2.4. Fourier transform infra-red (FTIR) spectroscopy: The samples were characterised by FTIR with Bomem MB 100 spectrometer. First, 1 mg of scraped sample were carefully mixed with 300 mg of potassium bromide, palletised under vacuum and characterised in the range of 500–4000 cm⁻¹ at the scan speed of 23 scan/min with 4 cm⁻¹ resolution.

2.5. UV-visible (Vis) analysis: UV-vis diffuse reflectance spectra of NPs were determined by UV-vis spectrophotometer (Avaspec-2048TEC s/n 0608052SI) to study their bandgap energy and UV-vis light absorption.

2.6. Scanning electron microscope: For characterising the morphology of the NPs scanning electron microscope (SEM) model Philips XL30 was used. To perform the electron microscopy imaging, samples were coated with a thin layer of gold by sputtering (EMITECH K450X, England) to promote electrical conductivity.

2.7. Transmission electron microscope: Transmission electron microscope (TEM) studies were performed with the Philips CM120 operated at 100 kV. The morphology and size of the synthesised NPs were assessed using TEM by dispersing in ethanol (0.1 g/10 ml) and ultrasound for 15 min. Finally, the samples were prepared by placing one drop of particles' dispersion on a carbon-coated grid.

2.8. Statistical analysis: All experiments were conducted in the fifth replicate. The results were given as means standard error. Statistical analysis was carried out by applying one-way analysis of variance and Tukey test with significance reported when $P < 0.05$. Also for study of group normalising, Kolmogorov–Smirnov test was used.

3. Results and discussion

3.1. Analysis of UV-vis and FTIR spectrums: FTIR spectra of the samples show strong interactions between Ag-NPs and gelatin molecules (Fig. 1a).

The FTIR spectrum for gelatin is a strong wide peak between 3000 and 3600 which is the index of tensile vibrations of N–H

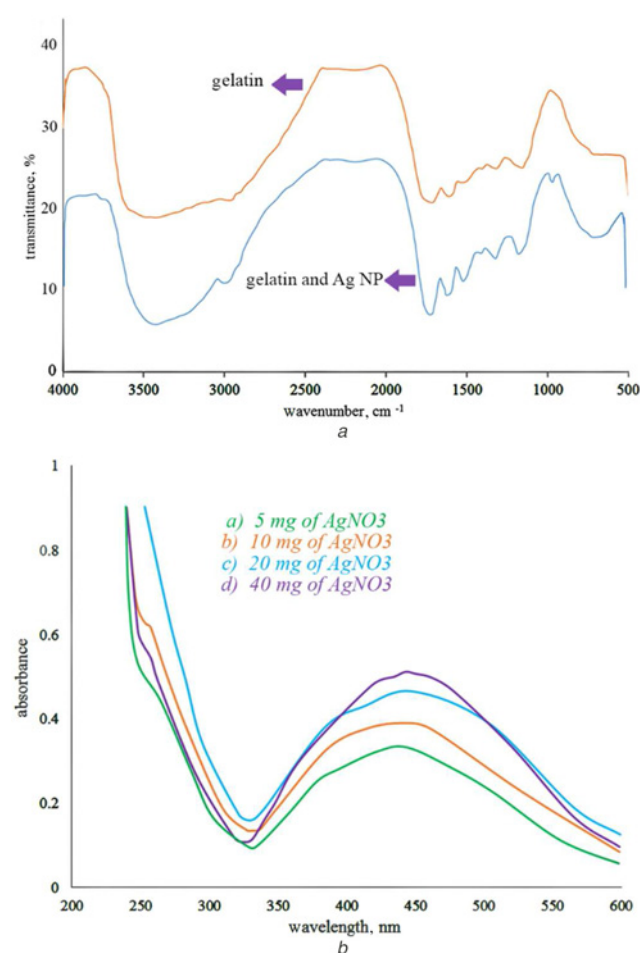


Fig. 1 Analysis of
a FTIR spectrum of gelatin and NPs
b UV-vis spectrum of NPs synthesised with gelatin

and O–H groups. Peaks between 1543 and 1651 relate to type 1 and type 2 amidic bonds of proteins, respectively. At 1348, there is a peak representing tensile vibrational C–N bonds in proteins. It can be seen that all peaks in the sample with gelatin and Ag-NPs are sharper and narrower which could be due to intermolecular hydrogen bonds of amine groups of gelatin having a greater tendency to form stronger bonds with metal atoms in the presence of Ag-NPs. FTIR spectrums of the samples prove strong interaction between NPs and proteins of gelatin.

The UV–vis spectrum of all four samples is presented in Fig. 1b, and as shown surface plasmon resonance (SPR) peak of Ag-NPs which is of their distinguishing indexes is between 437 and 449 complying with the orange–brown colour of mentioned NPs. There is always the possibility of UV–vis spectrum moving

upwards or downwards depending on SPR which in turn is affected by dielectric properties of coating material and of course shape and diameter of NPs.

3.2. Microscopic observations

3.2.1. Green synthesis: The thickness of gelatin coating was evaluated to be ~25 nm by analysing the shape of NPs (Fig. 2). In down to up method, nanomaterials formed by making blocks such as atoms and molecules bond perform self-assembly, that is, creation of molecules and macromolecules whose structural base is complex. Gelatin (protein)-coated Ag-NPs essentially form a mixed structure with high molecular weight thanks to the high tendency of protein molecules to self-assemble and creating heavy multi-molecular structures. Self-assembly of gelatin proteins occurs with that of NPs inside the proteins which could be associated with synergistic effect between metals and proteins to create multi-molecular structures. It has been proven that secondary interactions between proteins could play a significant role in structural agglomeration which is essentially a guided self-assembly process by gelatin's proteins.

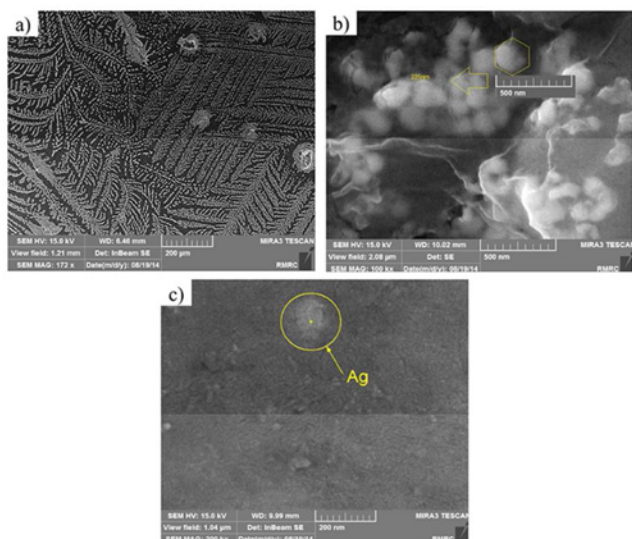


Fig. 2 SEM images of
a Self-assembly of Ag-NPs using gelatin
b Formed protein bridge in synthesis with gelatin (secondary self-assembly)
c Estimation of Ag-NP size in synthesis with gelatin (without gelatin coating thickness)

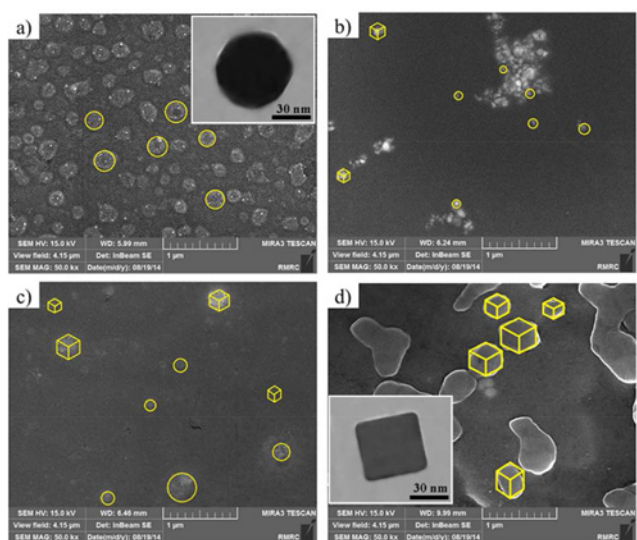


Fig. 3 Field-emission SEM images of green synthesis with gelatin after 72 h of exposure to sunlight (UV), indicating that as AgNO_3 increases gradually, the structures of NPs transform from
a Semi-spherical to
b Spherical–cubic
c Cubic–spherical and ultimately
d Semi-cubic morphologies. The insets are TEM images

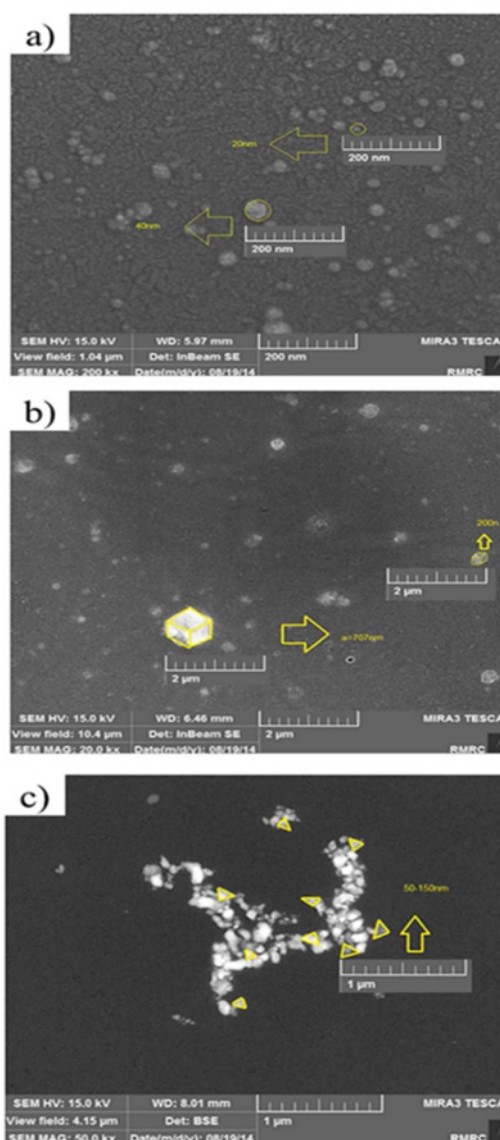


Fig. 4 SEM images of Ag-NPs with different shapes synthesised via chemical method indicating sodium borohydride as a strong reducer and consequently more oxidation of Ag particles to positive ions could result in
a Spherical NPs
b Cubic NPs that converted to
c Triangular NPs

Table 1 Antibacterial and antifungal properties of Ag-NPs synthesised by green and chemical synthesis

Synthesis method		Shape	<i>E. coli</i> MIC, µg/ml	<i>S. aureus</i> MIC, µg/ml	<i>C. albicans</i> MIC, µg/ml
green synthesis, mg AgNO ₃	5	spherical	15 **	15 **	12 *, **
	10	spherical–cubic	10	15	10
	20	spherical–cubic	8	12	5 *
	40	cubic	5	8	2 **
chemical synthesis		spherical	4 **	4 **	8
		triangular	2 **	4 **	2 **
		cubic	2 **	4 **	5 *

All experiments were conducted in the fifth replicate. Pairs that are significantly different from one another are marked by an asterisk (*), whereas * $P < 0.05$, ** $P < 0.01$ and *** $P < 0.001$.

The SEM images of four synthesised samples indicate that as AgNO₃ increases gradually, structures of NPs transform from spherical to spherical–cubic, cubic–spherical and ultimately cubic morphology (Fig. 3). The rapid increase of diameter in this synthesis could be associated with synergic effect of nanostructures with their coatings, hence creation of core/shell structures of NPs/gelatin. In a study, Darroudi *et al.* [19] have recently prepared Ag-NPs with simple and green synthesis method by reducing Ag⁺ ions in aqueous gelatin media, as a reducing and stabilising agent. They found that with increasing the temperature the size of NPs could be decreased. Moreover, the particle size of NPs obtained in gelatin solutions was smaller than in gelatin–glucose solutions, as a result of the rate of reduction reaction.

3.2.2. Chemical synthesis: In this Letter, spherical NPs could have been converted to triangular NPs, thanks to application of sodium borohydride as a strong reducer and consequently more oxidation of Ag particles to positive ions (Fig. 4). Also, the presence of oxygenated water alongside sodium citrate, sodium borohydride and piroyldon result in formation of triangular Ag-NPs. Colour transformation from yellow to blue could be associated with changes in plasmon resonance of surficial metallic nanostructures.

Changes in surface plasmon could be due to changes of surface angles caused by changes in adsorption by metallic molecules. Ag-NPs would be negatively charged due to adsorption of citrate ions causing repulsions between particles preventing agglomeration. Therefore, particles in solutions are stabilised without using any additional stabilising agent. However, to create ultrafine Ag-NPs sodium borohydride is used. The goal was to improve NP distribution which resulted in creation of ultrafine particles. Analysis of SEM images indicated formation of Ag-NPs in triangular, cubic and spherical shapes.

3.3. Antibacterial and antifungal test results

3.3.1. Green synthesis: Antibacterial properties of NPs were evaluated by MIC and minimum bactericidal concentration (MBC) tests. Different concentrations of Ag-NPs were used against negative-Gram bacteria *Escherichia coli* and positive-Gram bacteria *S. aureus* in LB broth. Bacterial growth was studied based on opacity of test tubes where transparency indicates growth cessation (bacteriostatic) or complete kill of bacteria. In case of bacteriostatic, if bacteria is cultured again it would grow again, whereas if they are killed no colony would be seen after culturing, due to which different values of MBC and MIC are obtained. MIC values against *S. aureus* are greater than those for *E. coli* due to a structurally superior cell wall in *S. aureus*. Killing tests were conducted against *E. coli* and MBC values were obtained by counting live bacteria in re-culturing in LB environment. First, the concentration in which no live bacteria is seen is taken as MBC value. MBC and MIC values for this Letter are the same, so MIC values are not presented. Changes of structural shapes from spherical to cubic, antibacterial properties of Ag-NPs

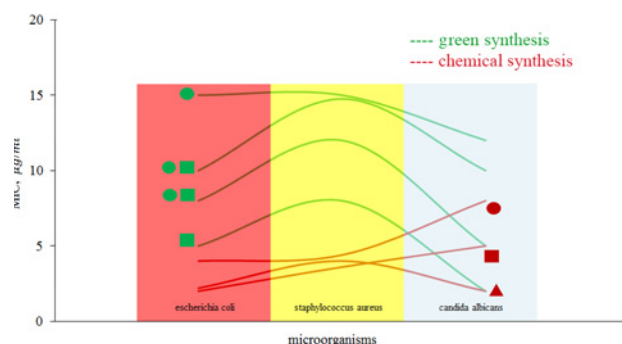


Fig. 5 Comparison of antibacterial and antifungal tests (MIC) in green and chemical synthesis. With change of structure for Ag-NPs from triangular to spherical antibacterial properties for both studied bacteria were decreased which could attest to the soundness of the proposed theorem. All experiments were conducted in the fifth replicate

were increased for both bacteria; since diameter changes are negligible, this fact serves as an evidence for effects of shape on antibacterial properties (Table 1). The antifungal properties of Ag-NPs were evaluated against *C. albicans* as presented, which showed properties at the level of one the best fungicides amphotericin-B with MIC value between 2.5 and 5 µg/ml. A comparative evaluation of our results and mentioned results in the literature shows that the green synthesised NPs have a relatively appropriate antibacterial activity for biomedical applications [20].

3.3.2. Chemical synthesis: A 5 µg/ml concentration of solution resulted in bacteriostatic conditions (opaque solution), whereas at 8 µg/ml bacteria were killed (transparent solution). With change of structure for Ag-NPs from triangular to spherical antibacterial properties for both studied bacteria were decreased which could attest to the soundness of the proposed theorem. Antifungal properties of the synthesised Ag-NPs were evaluated against *C. albicans* where NPs showed MIC values equal to 2–5 µg/ml. Minimum fungicidal concentration values obtained for 200 µg/ml concentration were much greater than MIC values a fact which is natural considering nature of membrane and wall of fungi (Table 1). The comparison of two methods on antibacterial and antifungal tests are shown in Fig. 5.

The strong interaction of Ag nanocrystals with gelatin molecules has been established long time ago. Since the first reports on this [21], many modified techniques have been proposed on different mechanisms for the interactive effects of Ag ions and gelatin molecules [22, 23]. Although our study suggests that the basic results are in agreement with the literature, the simplicity and efficacy of our technique make it favourable for many applications.

4. Conclusion: In this Letter, Ag-NPs were synthesised in spherical, cubic and triangular shapes using both chemical

and green synthesis methods. The latter is a very inexpensive method without using chemical reducers where the used bio-macromolecules were both acting as coating and stabilising agents. Moreover, they contributed to forming NPs and increasing antibacterial and antifungal properties. UV light of sunlight acted as the reducing agent. Finally, antibacterial and antifungal properties of NPs were evaluated and the corresponding results attested our theorem of shape of Ag-NPs affecting these properties.

5 References

- [1] Marambio-Jones C., Hoek E.M.V.: 'A review of the antibacterial effects of silver nanomaterials and potential implications for human health and the environment', *J. Nanoparticle Res.*, 2010, **12**, pp. 1531–1551, doi: 10.1007/s11051-010-9900-y
- [2] Ghafari Nazari A., Tahari A., Moztaazadeh F., *ET AL.*: 'Ion exchange behaviour of silver-doped apatite micro- and nanoparticles as antibacterial biomaterial', *Micro Nano Lett.*, 2011, **6**, p. 713
- [3] Elechiguerra J.L., Burt J.L., Morones J.R., *ET AL.*: 'Interaction of silver nanoparticles with HIV-1', *J. Nanobiotechnol.*, 2005, **3**, p. 6
- [4] Yazdanpanah A., Rezvani Z., Ramedani A., *ET AL.*: 'Nanobiomaterials set to revolutionize drug-delivery systems for the treatment of diabetes: state-of-the-art', in Grumezescu A.M.B. (ED.): 'Nanobiomaterials in drug delivery' (William Andrew Publishing, 2016, 1st edn.), pp. 487–514, doi: <http://dx.doi.org/10.1016/B978-0-323-42866-8.00014-9>
- [5] Martínez-Castañón G.A., Niño-Martínez N., Martínez-Gutiérrez F., *ET AL.*: 'Synthesis and antibacterial activity of silver nanoparticles with different sizes', *J. Nanoparticle Res.*, 2008, **10**, pp. 1343–1348, doi: 10.1007/s11051-008-9428-6
- [6] Sheehy K., Casey A., Murphy A., *ET AL.*: 'Antimicrobial properties of nano-silver: a cautionary approach to ionic interference', *J. Colloid Interface Sci.*, 2015, **443**, pp. 56–64
- [7] Bindhu M.R., Umadevi M.: 'Antibacterial and catalytic activities of green synthesized silver nanoparticles', *Spectrochim. Acta A, Mol. Biomol. Spectrosc.*, 2015, **135**, pp. 373–378
- [8] Wakshlak R.B.-K., Pedahzur R., Avnir D.: 'Antibacterial activity of silver-killed bacteria: the 'zombies' effect', *Sci. Rep.*, 2015, **5**, p. 9555
- [9] Velusamy P., Das J., Pachaiappan R., *ET AL.*: 'Greener approach for synthesis of antibacterial silver nanoparticles using aqueous solution of neem gum (*Azadirachta indica* L.)', *Ind. Crops Prod.*, 2015, **66**, pp. 103–109
- [10] Liu C.-H., Yu X.: 'Silver nanowire-based transparent, flexible, and conductive thin film', *Nanoscale Res. Lett.*, 2011, **6**, p. 75, Available at <http://www.nanoscalereslett.com/content/6/1/75>
- [11] Yazdanpanah A., Tahmasbi M., Amoabediny G., *ET AL.*: 'Fabrication and characterization of electrospun poly-L-lactide/gelatin graded tubular scaffolds: toward a new design for performance enhancement in vascular tissue engineering', *Prog. Nat. Sci. Mater. Int.*, 2015, **25**, pp. 405–413, doi: 10.1016/j.pnsc.2015.09.009
- [12] Ramedani A., Yazdanpanah A., Moztaazadeh F., *ET AL.*: 'On the use of nanoliposomes as soft templates for controlled nucleation and growth of hydroxyapatite nanocrystals under hydrothermal conditions', *Ceram. Int.*, 2014, **40**, pp. 1–5, doi: 10.1016/j.ceramint.2014.02.005
- [13] Coad B.R., Kidd S.E., Ellis D.H., *ET AL.*: 'Biomaterials surfaces capable of resisting fungal attachment and biofilm formation', *Biotechnol. Adv.*, 2014, **32**, pp. 296–307, doi: 10.1016/j.biotechadv.2013.10.015
- [14] Cao S., Liu B., Fan L., *ET AL.*: 'Highly antibacterial activity of N-doped TiO₂ thin films coated on stainless steel brackets under visible light irradiation', *Appl. Surf. Sci.*, 2014, **309**, pp. 119–127, doi: 10.1016/j.apsusc.2014.04.198
- [15] Rostami A., Mozafari M., Gholipourmalekabadi M., *ET AL.*: 'Optimization of fluoride-containing bioactive glasses as a novel scoliotic agent adjunct to hydatid surgery', *Acta Trop.*, 2015, **148**, pp. 105–114, doi: 10.1016/j.actatropica.2015.04.021
- [16] Le Ouay B., Stellacci F.: 'Antibacterial activity of silver nanoparticles: a surface science insight', *Nano Today*, 2015, **10**, pp. 339–354, doi: 10.1016/j.nantod.2015.04.002
- [17] Rathi Sre P.R., Reka M., Poovazhagi R., *ET AL.*: 'Antibacterial and cytotoxic effect of biologically synthesized silver nanoparticles using aqueous root extract of *Erythrina indica* lam', *Spectrochim. Acta A, Mol. Biomol. Spectrosc.*, 2015, **135**, pp. 1137–1144
- [18] Franci G., Falanga A., Galdiero S., *ET AL.*: 'Silver nanoparticles as potential antibacterial agents', *Molecules*, 2015, **20**, pp. 8856–8874, doi: 10.3390/molecules20058856
- [19] Darroudi M., Bin Ahmad M., Abdullah A.H., *ET AL.*: 'Green synthesis and characterization of gelatin-based and sugar-reduced silver nanoparticles', *Int. J. Nanomed.*, 2011, **6**, (1), pp. 569–574
- [20] Naddeo J.J., Ratti M., O'Malley S.M., *ET AL.*: 'Antibacterial properties of nanoparticles: a comparative review of chemically synthesized and laser-generated particles', *Adv. Sci. Eng. Med.*, 2015, **7**, (12), pp. 1044–1057
- [21] James T.H.: 'The theory of the photographic process hardcover' (Macmillan Pub. Co., 1977, 4th edn.), p. 715, ISBN-10: 0023601906
- [22] Sondi I., Salopek-Sondi B.: 'Silver nanoparticles as antimicrobial agent: a case study on *E. coli* as a model for Gram-negative bacteria', *J. Colloid Interface Sci.*, 2004, **275**, (1), pp. 177–182
- [23] Seth D., Choudhury S.R., Pradhan S., *ET AL.*: 'Nature-inspired novel drug design paradigm using nanosilver: efficacy on multi-drug-resistant clinical isolates of tuberculosis', *Curr. Microbiol.*, 2011, **62**, (3), pp. 715–726